LLNL-CONF-415167

Insulator Surface Flashover Due to UV Illumination

J. B. Javedani, T. L. Houck, D. A. Lahowe, G. E. Vogtlin, D. A. Goerz

July 29, 2009

17th IEEE International Pulsed Power Conference
Washington D.C., DC, United States
June 28, 2009 through July 2, 2009

Insulator Surface Flashover Due to UV Illumination

J. B. Javedani, T.L. Houck, D.A. Lahowe, G.E. Vogtlin and D.A. Goerz
Lawrence Livermore National Laboratory, L-154
7000 East Avenue, Livermore, CA, USA

Abstract

The surface of an insulator under vacuum and under electrical charge will flashover when illuminated by a critical dose of ultra-violet (UV) radiation - depending on the insulator size and material, insulator cone angle, the applied voltage and insulator shot-history. A testbed comprised of an excimer laser (KrF, 248 nm, ~16 MW, 30 ns FWHM,), a vacuum chamber, and a negative polarity dc high voltage power supply (≤ -60 kV) were assembled to test 1.0 cm thick angled insulators for surface-flashover. Several candidate insulator materials, e.g. High Density Polyethylene (HDPE), Rexolite^R 1400, Macor^{TM} and Mycalex, of varying cone angles were tested against UV illumination. Commercial energy meters were used to measure the UV fluence of the pulsed laser beam. In-house designed and fabricated capacitive probes (D-dots, >12 GHz bandwidth) were embedded in the anode electrode underneath the insulator to determine the time of UV arrival and time of flashover. Of the tested insulators, the +45 degree Rexolite insulator showed more resistance to UV for surface flashover; at UV fluence level of less than13 mJ/cm^2, it was not possible to induce a flashover for up to -60 kV of DC potential across the insulator's surface. The probes also permitted the electrical charge on the insulator before and after flashover to be inferred. Photon to electron conversion efficiency for the surface of Rexolite insulator was determined from charge-balance equation. In order to understand the physical mechanism leading to flashover, we further experimented with the +45 degree Rexolite insulator by masking portions of the UV beam to illuminate only a section of the insulator surface; 1) the half nearest the cathode and subsequently, 2) the half nearest the anode. The critical UV fluence and time to flashover were measured and the results in each case were then compared with the base case of full-beam illumination. It was discovered that the time for the insulator to flash was earlier in time for the cathode-half beam illumination case than the anode-half illumination case which led us to believe that the flashover mechanism for the UV illumination is initiated from the cathode side of the insulator. Qualitatively stated, the testing revealed that the shielding of the cathode triple point against UV is more important than the anode triple junction in the design of vacuum insulators and electrodes.

I. Objectives

The goal of this work was to acquire empirical data on critical UV fluence (energy per unit area) required to induce surface flashover of vacuum insulators for some candid insulator materials: High Density Polyethylene (HDPE), Rexolite^R 1400, Macor^{TM} and Mycalex. This work was a clarification and extension of studies performed by C.L. Enloe, et. al. in the 80's [1-3]. Additionally, to gain an understanding of the physical mechanism of flashover, we experimented with UV illumination of a portion of the insulator's surface near the cathode and subsequently near the anode. The results of these experiments are covered in detail.

II. UV-Insulator Testbed

Photographs of the UV-Insulator Testbed showing the opened vacuum chamber, electrodes, and test insulator are shown in Figures 1 and 2. The vacuum chamber containing the insulator was kept under high vacuum (micro torr). The vacuum system consisted of a small mechanical roughing pump and a CTI^{TM} cryopump (CTI Cryogenics/Helix, Model: Cryo Torr 8). The potential across the insulator, i.e. between the electrodes, could be adjusted up to -60 kV with a variable dc voltage supply connected through a 5 MΩ isolation/limiting resistor to the cathode. The power supply was electronically disconnected when the laser was pulsed. Insulators tested included High Density Polyethylene (HDPE), Rexolite, Macor and Mycalex of varying cut angles (0^0, $\mp 30^0$ and $\mp 45^0$).

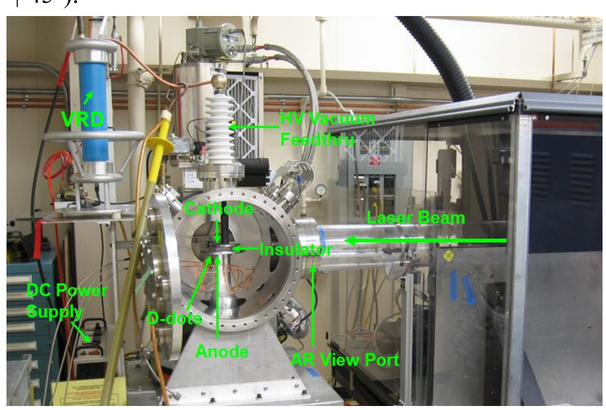

Figure 1. A photo of the UV-Insulator Testbed.

This work performed under the auspices of the U.S. Department of Energy by Lawrence Livermore National Laboratory under Contract DE-AC52-07NA27344.
Email: javedani1@llnl.gov

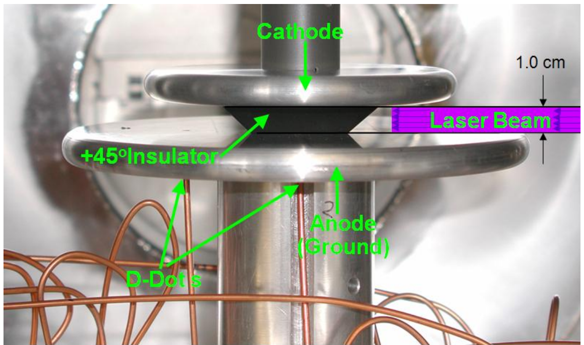

Figure 2. A photo of a +45^0 insulator under test.

A commercial excimer laser located adjacent to the vacuum chamber was the source of UV photons. The specs for the laser were; Lambda Physik (LPX 325i), krF, 248 nm, ~16 MW, 30 ns FWHM. The laser beam was masked so that it had a 1.0 cm by 1.0 cm square cross section at the test insulator . The illumination area consisted of a 1-cm wide strip extending from the cathode to anode. A schematic of the optical beam line between the laser and insulator is provided in Figure 3.

A photodiode registered the temporal shape of the pulse and a commercial energy meter determined the energy of the pulse at the insulator. The laser energy is variable by adjusting the voltage of the thyratron output switch (13 kV to 19 kV) and was capable of delivering up to 75 mJ/cm^2 on the surface of the insulator. Neutral density filters were used for larger energy variations.

The laser was nominally operated with the thyratron output switch set at 18 kV and single pulse mode. Figure 4 shows three typical laser power output waveforms and the corresponding UV energy at the insulator.

Fast capacitive probes, produced in-house and referred to as D-dots in this article, were embedded in the anode (ground) electrode to provide temporal data on arrival time of the laser pulse and surface flashover time. The laser power waveform between these two times was integrated over time to yield the critical energy, refer to Section III. The probes also gave information that permitted the electrical charging of the insulator during illumination to be inferred.

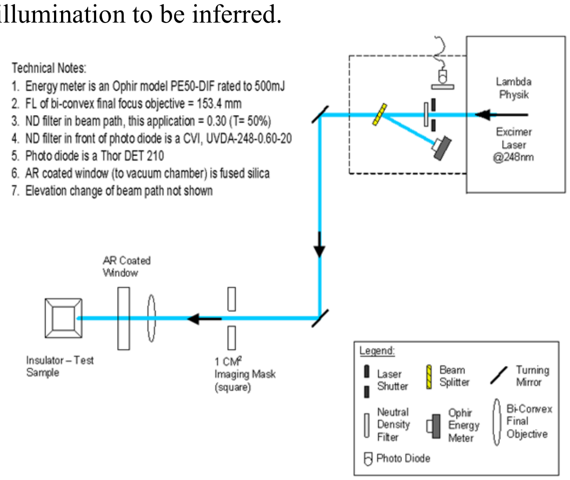

Figure 3. Sketch of the laser beam path to insulator.

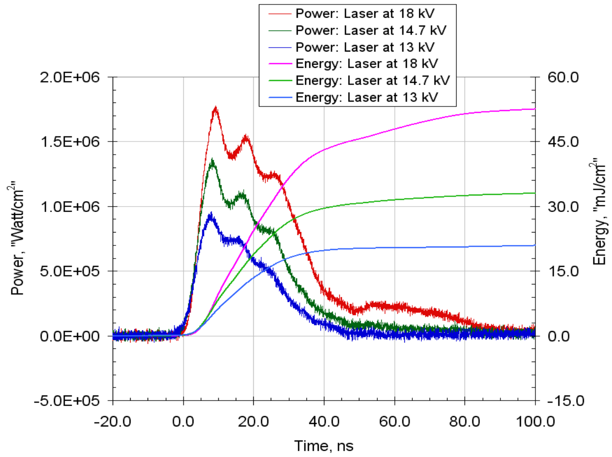

Figure 4. Laser output waveforms; power and energy.

III. D-Dot Probes

The capacitive probes were developed in-house for this specific application and are described in detail elsewhere [4]. Due to the importance of this diagnostic for this paper, a brief summary of capacitive probe concept and its operation is given. This diagnostic is based on the principle of capacitive coupling and is known as a D-dot probe due to its sensitivity to the changing of the electric displacement field. The probe in the final form, in our design, was the tip of small coaxial cable (RG-405/U) that was inserted in the anode (grounded) electrode with its surface flush with the interior side of the electrode. The surface of the inner electrode of the coax couples to the electrical field of the driving electrode through a capacitance, C_c and is also coupled to the much smaller electrical field between the probe and the wall (grounded electrically) through a capacitance C_w. A lumped circuit model of a D-dot probe is shown in Figure 5. In the figure, V_S is the signal registered on the scope by the probe due to the electrodes drive voltage, V_D.

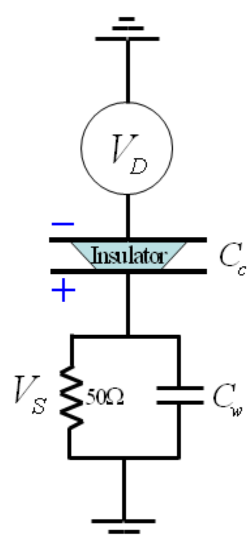

Figure 5: Lumped element circuit model of D-dot.

From applying Kirchhoff's voltage law to the circuit and conservation of charge the relationship between V_S and V_D can be derived as:

$$V_D(t) = \frac{C_c + C_w}{C_c} V_S(t) + \frac{1}{ZC_c} \int_0^t V_S(t')\ dt' + V_D(0) \qquad (1)$$

Z is the output impedance of the registering scope and $V_D\,(0)$ is the initial potential on the cathode. There were two key design parameters for the D-dots; 1) the magnitude of the probe's signal, V_S and 2) the bandwidth of the probe. It can be shown that the magnitude of V_S is proportional C_c and the bandwidth of the probe is determined from the sum of C_c and C_w. Correct choosing of the probe size would mean that the signal is strong enough that does not to be amplified or attenuated during testing. The ratio of V_S to V_D in this application is ~$10^{-4.}$ Note that C_c is related to the total geometry especially the spacing between the electrodes which is best estimated with computational modeling and C_w depends primarily on the dimensions of the probe.

Multiple probes were embedded in the anode (ground) for the insulator testing to permit location of the flashover site from time of flight comparison. As mentioned previously, the probes provided the UV arrival time on the insulator and the time of flashover. In Figure 2, the semi-rigid copper-jacketed coaxial cables visible below the electrodes connect the D-dots to a Tektronix TDS6124C, 12 GHz oscilloscope. In deriving Equation (1), we assumed that the electrical field is due only to the potential difference of the probe to the cathode and wall (anode). However, charge due to photoemission from the insulator surface will alter the local electrical field inducing a charge on the probe. One of the probes – the one nearest the illuminated insulator surface – was able to detect the charging of the insulator surface by UV illumination as a prelude to the insulator flashover. The signals from these probes are explained in the next section.

IV. Full Surface Illumination Measurements

Measurements of UV energy to induce flashover were taken for insulator angles of 0, ±30, and ±45 degrees for HDPE, Rexolite® 1400, Macor™ and Mycalex. Over 3000 shots were recorded. A precision mask in the beam path was used to define an area 1-cm wide and extending from the cathode to the anode that was illuminated on the insulator surface. Up to 75 mJ/cm^2 of ~5 eV photons was deposited on the insulator during a pulse. Electrode charging voltage was varied up to a maximum of 60 kV.

A typical test-run started with establishing the self-break voltage on the insulator; for example, 45° insulators showed the highest self-break voltage (~60 kV) while 0 degree showed the lowest (~40 kV) for Rexolite. The UV pulse energy, waveform and the time

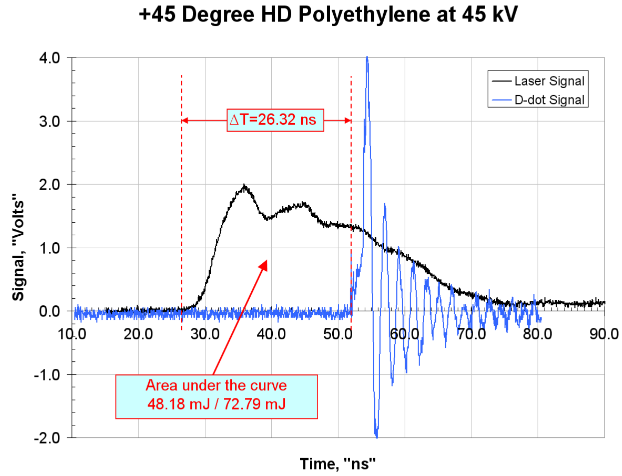

Figure 6. D-dot signal during flashover and laser power signal.

to flashover was recorded as the voltage was reduced in increments of 2.5 kV.

It is assumed any charge deposited on the insulator was fully discharged during a flashover leaving no residue charge to part take in the next shot.

The digitizing oscilloscope was triggered by the signal from the photo diode. Signals from the D-dot probes were also recorded on the oscilloscope to permit the determination of time to flashover after arrival of the UV pulse at the insulator. The temporal shape, $f\,(\tau)$ of the laser pulse was relatively constant from shot to shot. To calculate the critical fluence we normalized the integrated diode pulse, i.e.

$$\int_0^\infty f\ \ \tau\ \ d\tau = 1 \qquad (2)$$

and then defined the critical fluence, F_C, as;

$$F_C \equiv \frac{E}{A} \int_0^{t_f} f\ \ \tau\ \ d\tau \qquad (3)$$

Where E is the total pulse energy, A is the cross sectional area of the beam and t_f is the time delay from first illumination until flashover. Thus, the critical fluence is the total energy deposited on the insulator before flashover divided by the area of the beam. Note this area is only equal to the illuminated area for the 0° insulator. Figure 6, shows the time corrected raw signals of the photo diode and the D-dot during flashover for the case of +45° insulator illuminated by a 73 mJ/cm^2 laser pulse. In that case the Critical fluence, F_c, was 48 mJ/cm^2.

Figure 7 shows typical signals from two of the probes. D-dot1 is the probe located nearest the illuminated surface and D-dot2 is any of the other probes – far away from the surface of the insulator that has gone through flashover.

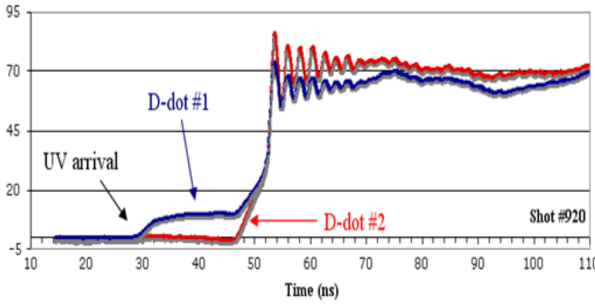

Figure 7: Integrated raw D-dot Probe signals.

V. Insulator Charging

The temporal data of the D-dots is used to determine the critical energy needed for flashover. But the probe data also permits an estimate of the photon-to-electron conversion efficiency and the critical electrical charge on the insulator for flashover. Figure 8a shows the response of a D-dot probe for shot 2757. Figure 8b shows the corresponding time of laser photon output. Upon the arrival of UV at the insulator surface the probe records a change in the electrical field. We deduce that this change is caused by charge buildup on the insulator surface as the potential between the electrodes remains constant. Mathematically we can express this surface charging as:

$$\frac{dQ}{dt} = \alpha\ I(t) - Q(t)/\beta \qquad for \quad t_0 < t \le t_{br} \tag{4}$$

Where $Q\ (t)$ is the charge on the insulator, $I\ (t)$ is the intensity of the UV beam in photons/sec. Thus, $\alpha I\ (t)$ is the rate that the UV produces photoelectrons. As the photoelectrons are swept away from the insulator by the electric field, the surface will develop an increasing positive charge. This surface charging will change the local electric field eventually preventing further charging. This effect is represented by the $Q\ (t)/\beta$ term. α And β are constants. The initial rate of charging and steady state charge of the insulator surface is needed to determine α and β. This requires calibrating the measured charge on the probe to the corresponding charge on the insulator.

The determination of this calibration of insulator charge to the induced probe charge is somewhat involved. The charge is not expected to be distributed uniformly along the surface. As an approximation, we assume a non-uniform distribution weighted as a function of the normal component of the electrostatic field, E_n, for the case of no charging. Given this assumption, a 3D electrostatic model was created of the insulator. In this model the 1.0-cm wide strip of irradiated insulator surface was divided into 16 bins (10

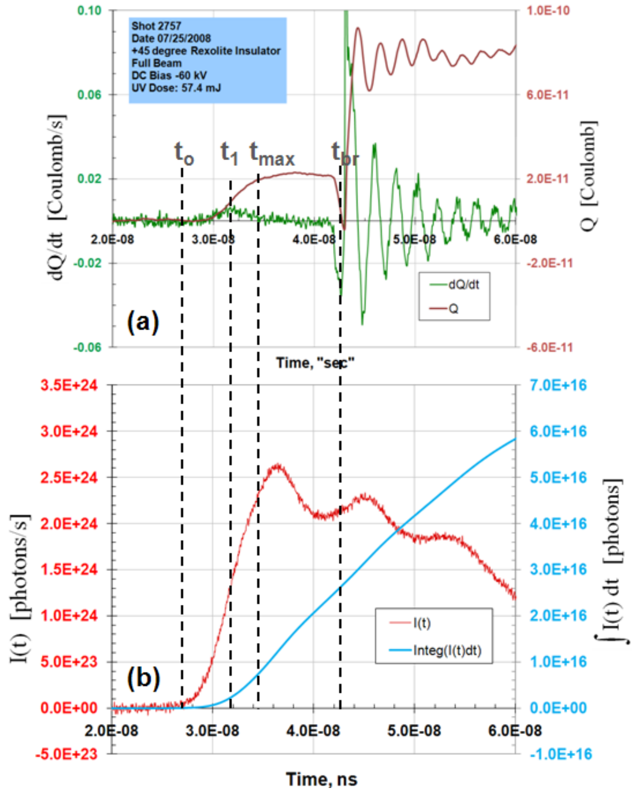

Figure 8: (a) D-dot signal and (b) laser signal corresponding to Shot 2757.

mm wide by 0.9 mm height by 0.5 mm deep) between the anode and cathode. Each bin was then filled with positive charge according to the E_n weighting until the difference between probe 1 and probe 2 agreed with ~20 pC shown in Figure (9). It was found that a charge of ~67 nC was required on the insulator to produce the measured ~20 pC differential charge between the probes (probe1 at 14.3 pC and probe2 at 34.3 pC). The ratio between the charge on the insulator Q, to the charge on the probe q, can be thought of a geometrical factor g,

$$g = \frac{Q}{q} = \frac{67\ \text{nC}}{20\ \text{pC}} = 3.35\times 10^3 \tag{5}$$

A. Calculation of α

Initially for $t < t_1$, equation (4) for the insulator can be rewritten as;

$$\frac{dQ}{dt} = \alpha\ I(t) \qquad for \quad t_0 < t \le t_1 \tag{6}$$

Substituting Equation (5) into Equation (6) and solving for α:

$$\alpha = \frac{dq/dt}{I(t)}\, g = \frac{5\times 10^{-3}\,\text{C/s}}{1\times 10^{24}\ \text{photon/s}}\, 3.35\times 10^3 \tag{7}$$

$$\alpha = 1.67\times 10^{-23}\,\frac{\text{C}}{\text{photon}} = 1.04\times 10^{-4}\,\frac{\text{electron}}{\text{photon}}$$

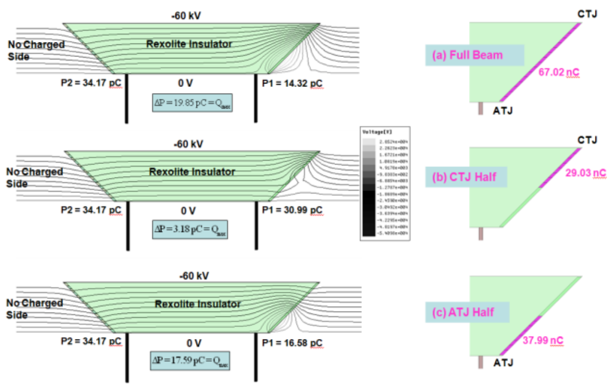

Figure9: Estimate of positive charge on the insulator at the time of flashover – via modeling.

In other words, it takes ~10,000 photons (~ 5 eV) to create 1 electron on the surface of the Rexolite insulator.

B. *Calculation of β*

Constant β can be calculated for the time that $dQ/dt = 0$ in equation (4), i.e., $t_{max}<t<t_{br}$.

Again for the example shot 2757 in Figure 8:

$$\beta = \frac{\int_{t_{max}}^{t_{br}} q(t)\ dt}{\alpha \int_{t_{max}}^{t_{br}} I(t)\ dt} g = \frac{2.1\times 10^{-11} * 9\times 10^{-9}}{1.67\times 10^{-23} * 2.0\times 10^{16}} 3.35\times 10^{3} \qquad (7)$$

$$\beta = 1.9\times 10^{-9}\ \text{sec}$$

Knowing the constants α and β, Equation (4) can be rewritten:

$$\frac{dQ}{dt} = 1.67\times 10^{-23} I(t) - \frac{Q(t)}{1.9\times 10^{-9}} \quad for\ t_0 < t \le t_{br}$$

IC: Q(0) = 0 (8)

An examination of data for other cases shows that α remains constant while β linearly increases with the applied biased field.

VI. Partial Surface Illumination Measurement

The Critical UV fluence results for HDPE, Rexolite, Macor and Mycalex has been published elsewhere [5]. The +45^{o} Rexolite showed slightly better flashover resistance to UV illumination than other tested materials.

Here, we report on the results that were obtained when the laser beam was masked so that only half of the beam illuminated the cathode side and conversely when the beam illuminated the anode side. The fluence data for the three case of 1) Full beam illumination of insulator surface, 2) Half beam illumination of the cathode half of the insulator surface and 3) Half beam illumination of the anode half of the insulator surface is shown in

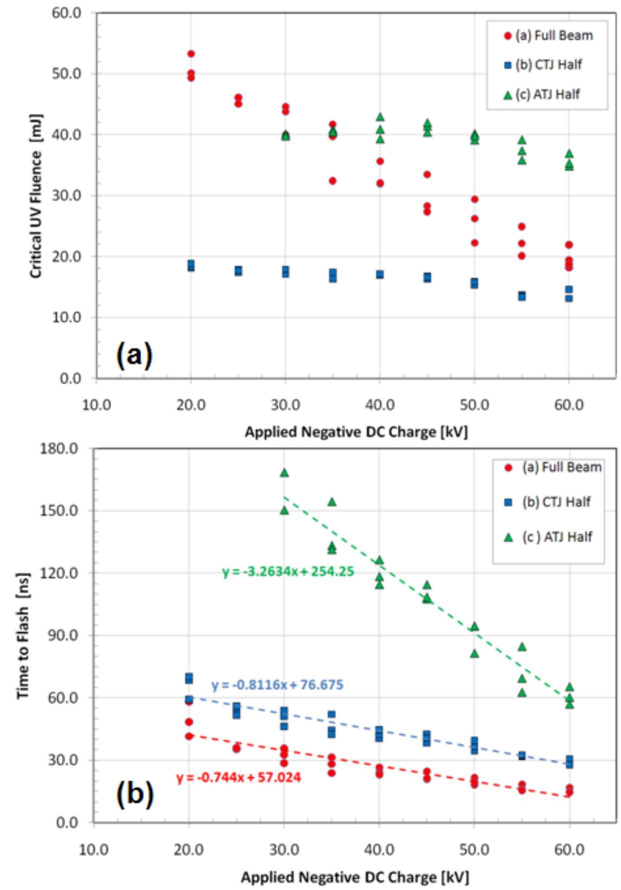

Figure10: (a) UV fluence data and (b)time to flash data for Full-beam, cathode-half and anode-half UV Illumination .

Figure 10, the average incident UV energy was about 58 mJ, 21 mJ and 40 mJ for each case respectively.

Several observations were made.

1. The beam UV power was not uniform – anode side illumination sees 68% of the energy.
2. The higher was the biased DC voltage the earlier the breakdown for all cases.
3. For cathode-side-illumination case, the probe did not detect its usual "bump" in charge due to UV arrival – simply because the probe was too far away from event.
4. Breakdown occurred sooner for the cathode-side-illumination case than the anode side; cathode-side-illumination breakdown occurred nearly as early as the full-beam case. *Cathode-side-illumination was thus the UV initiation site for flashover.*
5. Anode-side-illumination flashover occurred later in time, with 10's of ns delay, and requires surface charging thus depends on the insulator length.

VII. Modeling Partial Illumination

By turning off the top half bins (set to zero) in the 3D model, the cathode side illumination test was simulated. By turning off the bottom half bins the anode side illumination test was simulated. The charge difference between the probes was checked again in the model and was in good agreement with the actual test for the half beam cases. Figure 9 shows the results of the simulation. The charge on the insulator in all three cases disturbed the background equipotential lines so that some of the lines impinged the surface at the undesired angle of 90^o. It was estimated that as much as 29 nC of positive charge was deposited on the cathode half and 38 nC on the anode half of the insulator at the time of flashover.

VIII. Summary

A testbed was assembled to test insulators under vacuum and under DC charge for UV-induced flashover. The UV source was a 5 eV excimer laser capable of outputting single bursts of photons (up to 75 mJ/cm^2 of 30 ns FWHM and 1.0 cm by 1.0 cm beam cross section). Critical UV energy was measured for insulator flashover for various insulator materials (HDPE, Rexolite, Mycalex and Macor) with varying angles (0, 30 and 45) as a function of biased (negative) voltage. Rexolite did better in resisting UV; no flashover was observed at less than 13 mJ/cm^2 for the 0-to-60 kV of applied biased voltage. Insulator charge balance equation was derived from the D-dot probe data and an assumption on the ratio of the insulator charge to that of the probe based on a computational model. From the charge balance equation it is estimated that it took about 10,000 photons to create an electron on the surface of the insulator for a typical example with $+45^o$ Rexolite insulator.

The laser beam was then masked so that only the top of the insulator (cathode side) was exposed to UV and to compare the beam was also masked so that the bottom side of the insulator (anode side) was exposed to UV. The breakdown occurred sooner for the cathode side illumination that the anode side illumination - it was nearly as early as the full beam illumination case. It was inferred that the cathode triple junction is the initiation site for flashover and was included that it is more important to shield the cathode triple point against UV in the design of vacuum insulators.

ACKNOWLEDGMENT

We like to thank Mr. Tony Ferriera, Mr. Greg Hawkins and Mr. Jim Crawford in mechanical support and Mr. Ronnie Speer and Mr. John Taylor in electrical support of the experiment.

REFERENCES

[1] C. Enloe, et al., “Vacuum Ultra-Violet Effects on Power Transport Across a Vacuum/Solid Dielectric Interface,” in *Proc. X^{th} International Symposium on Discharges and Electrical Insulation in Vacuum*, vol. I (Columbia, SC), Oct. 1982, pp. 308-314.

[2] C. L. Enloe and R. E. Reinovsky, "Ultra-violet induced insulator flashover as a function of material properties", Proceedings of the 4^{th} International IEEE Pulsed Power Conference, p. 679 (1983).

[3] C.L. Enloe and R.M. Gilgenbach, “Microscopic and Macroscopic Material Property Effects on Ultraviolet-Laser-Induced Flashover of Angled Insulators in Vacuum,” *IEEE Trans.Plasma Sci*., vol. 16 no. 3, June 1988, pp. 379-389.

[4] T.L. Houck, et. al. “Fast Diagnostic For Electrical Breakdowns in Vacuum”, LLNL-TR-402609, March 2008.

[5] J.B. Javedani, et. al. “Ultra-Violet Induced Insulator Flashover” 28^{th} IEEE International Power Modulator Symposium and 2008 High Voltage Workshop, Las Vegas, NV, pp. 33-36.